JASA ARTICLE

Temperature-driven seasonal and longer term changes in spatially averaged deep ocean ambient sound at frequencies 63–125 Hz

Michael A. Ainslie,[1,a)] Rex K. Andrew,[2] Bruce M. Howe,[3,b)] and James A. Mercer[2]
[1]*JASCO Applied Sciences (Deutschland) GmbH, Mergenthaler Allee 15-21, 65760 Eschborn, Hesse, Germany*
[2]*Applied Physics Laboratory, University of Washington, Seattle, Washington 98105, USA*
[3]*University of Hawaii at Manoa, Honolulu, Hawaii 96822, USA*

ABSTRACT:
The soundscape of the Northeast Pacific Ocean is studied with emphasis on frequencies in the range 63–125 Hz. A 34-year (1964–1998) increase and seasonal fluctuations (1994–2006) are investigated. This is achieved by developing a simple relationship between the total radiated power of all ocean sound sources and the spatially averaged mean-square sound pressure in terms of the average source factor, source depth, and sea surface temperature (SST). The formula so derived is used to predict fluctuations in the sound level in the range 63–125 Hz with an amplitude of 1.2 dB and a period of 1 year associated with seasonal variations in the SST, which controls the amount of sound energy trapped in the sound fixing and ranging (SOFAR) channel. Also investigated is an observed 5 dB increase in the same frequency range in the Northeast Pacific Ocean during the late 20th century [Andrew, Howe, Mercer, and Dzieciuch (**2002**). ARLO **3**, 65–70]. The increase is explained by the increase in the total number of ocean-going ships and their average gross tonnage. © *2021 Acoustical Society of America*. https://doi.org/10.1121/10.0003960

(Received 1 October 2020; revised 12 February 2021; accepted 11 March 2021; published online 12 April 2021)
[Editor: D. Benjamin Reeder] Pages: 2531–2545

I. INTRODUCTION

Anthropogenic sound in the ocean is a growing source of concern because of its possible detrimental effect on marine life such as marine mammals (Richardson *et al.*, 1995; Southall *et al.*, 2007; Southall *et al.*, 2019) and fish (Slabbekoorn *et al.*, 2010; Popper *et al.*, 2014). Human activities that produce underwater sound include seismic surveys with airgun arrays (International Association of Oil and Gas Producers, 2011) and global commercial and industrial shipping (Hildebrand, 2009, Frisk, 2012). Sertlek *et al.* (2019) estimates that approximately 83% (0.88 out of 1.07 pJ/m^3) of sound energy above 100 Hz in the Dutch North Sea originates from shipping, followed by 16% from seismic surveys, 1% from explosions [controlled detonations of World War 2 ordnance], and less than 1% from wind. Although these values do not apply to a deep ocean scenario, they indicate the importance of anthropogenic sources in a modern soundscape and illustrate the benefits of an energetic approach to ocean sound budgets.

Increases in deep water ocean sound levels have been estimated as large as 0.5 decibels per year (dB/a) on average between 1950 and 1970 at 50 Hz (Ross, 1974) and about 0.3 dB/a between 1950 and 2007 in the frequency band 25–50 Hz (Frisk, 2012). Spectral density levels of low frequency sound in the Northeast Pacific Ocean in the frequency range 16–100 Hz increased by between 3 and 12 dB—depending on the frequency and location—from the mid-1960s to the end of the 20th century (Andrew *et al.*, 2002; McDonald *et al.*, 2006; Andrew *et al.*, 2011; Chapman and Price, 2011). This increase has been widely attributed to shipping (Andrew *et al.*, 2002; McDonald *et al.*, 2006; Andrew *et al.*, 2011; Frisk, 2012) No further increase was observed, on average, following continuous monitoring at the same locations during the shorter period 1994–2007 (Andrew *et al.*, 2011). The continuous monitoring revealed an annual cycle attributed to baleen whale migrations in the frequency band 16–20 Hz and seasonal weather patterns at higher frequency (63–100 Hz).

Part of the 1965–2000 increase in the Northeast Pacific can be explained by a 2% per year average increase in the number of large ships (doubling in 35 years; see Fig. 1), which, in the absence of other changes (and assuming an incoherent addition of radiated sound power) would explain a total increase of about 3 dB in 35 years. The average gross tonnage per ship increased by 1.5% per year (two thirds increase in 35 years) during the same period (Hildebrand, 2009), suggesting that part of the missing 0–9 dB (the part of the 9–12 dB increase not explained by the 3 dB associated with the increased number of ships) might be related to an increase in the average size or propulsion power of shipping vessels. McDonald *et al.* (2006) argue that higher source

[a)]Also at: Institute of Sound and Vibration Research, University of Southampton, UK. Electronic mail: michael.ainslie@jasco.com, ORCID: 0000-0002-0565-3559.
[b)]ORCID: 0000-0001-5711-5253.

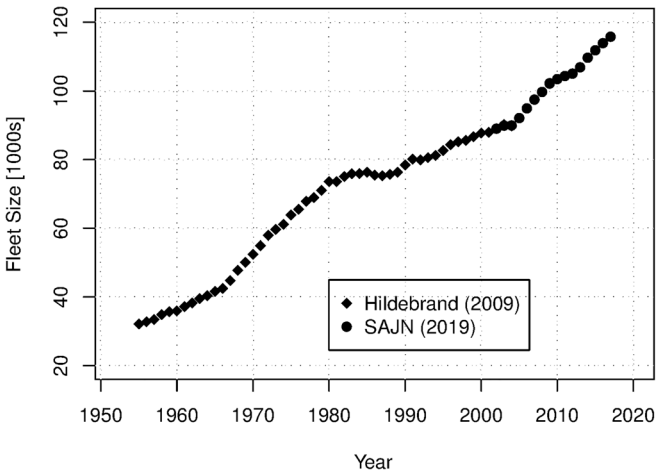

FIG. 1. Size of global shipping fleet according to Hildebrand (2009) and Shipbuilders' Association of Japan (2019).

levels of "at least some of the vessels are needed to explain the additional 7–9 dB increase in the 30–50 Hz band."

Increasing acoustic transparency due to acidification has been proposed as a possible cause of increasing ocean sound (Hester *et al.*, 2008, Brewer and Hester, 2009) but this mechanism is considered unlikely to lead to a significant contribution (Rouseff and Tang, 2010; Joseph and Chiu, 2010; Udovydchenkov *et al.*, 2010). The frequency range in which the 1965–2000 increase is largest (30–40 Hz) is also occupied by baleen whale vocalizations (Curtis *et al.*, 1999; Burtenshaw *et al.*, 2004; McDonald *et al.*, 2008). It is, therefore, possible that in this frequency range, the increase is partly or mostly due to a change in the number or geographical distribution of vocalizing whales, the call rate or intensity, or some combination of these.

The focus of the present work is on explaining the observed seasonal and long-term (multi-decadal) changes in the Northeast Pacific Ocean and, in particular, on the contribution from shipping between 63 and 125 Hz. In addition to the number of ships (M), changes in ship tonnage (g), and sea surface temperature (SST) are considered as potential factors affecting the increase. In particular, we hypothesize that

- the long-term trend can be explained by changes in M and g alone with no change in the source level; and
- the seasonal fluctuations can be explained by changes in SST alone.

The rest of the paper is structured as follows. A theoretical formula for spatially averaged mean-square sound pressure (saMSP) is derived in Sec. II for near-surface sound sources such as ships. The resulting expression depends on the source level, depth, and number of sound sources, the attenuation coefficient of seawater, and the SST. Measurements of ambient sound spectra recorded at a number of deep water receivers close to the North American Pacific coast from (Andrew *et al.*, 2011) in a frequency range normally attributed to shipping sound are summarized in Sec. III, and assumed properties of the sound sources and propagation medium are described in Sec. IV. Theoretical predictions are compared with measurements in Sec. V, using an average over multiple receivers as a proxy for a global average, and an explanation is suggested for seasonal variations in saMSP in terms of the corresponding seasonal fluctuations in the SST. A summary and discussion in Sec. V is followed by conclusions in Sec. VI.

Acoustical terminology follows ISO (2017).

II. THEORY: AVERAGE SOUND FIELD (MULTIPLE SOURCES)

A. Sound energy density and mean-square sound pressure

The contribution of a large number of individual sound sources to the mean-square sound pressure (MSP) at some fixed location can be estimated by considering an enclosed region of space filled with a large number of sources, the ith of which makes a contribution H_i to the total sound energy such that the total energy (in joules) added over the entire volume is

$$H_{\text{tot}} = \sum_i H_i. \tag{1}$$

In a medium of speed of sound c and density ρ, the energy density of the sound field is related to the MSP according to Pierce (1989)

$$H_V = \frac{\overline{p^2}}{\rho c^2}, \tag{2}$$

where the overbar indicates an average over time. Assuming spherical spreading, the MSP at a distance r from a point source of power W is

$$\overline{p^2} = \frac{\rho c}{4\pi}\frac{W}{r^2}\exp(-2\alpha r), \tag{3}$$

where α is the absorption coefficient.

Substituting Eq. (3) in Eq. (2), integrating the energy density over all space, and assuming the total acoustic energy H is twice the potential energy gives (Ainslie *et al.*, 2009)

$$H = \frac{W}{2\alpha c}. \tag{4}$$

It is convenient to introduce the equivalent free-field sound power, ΔW_i, defined as the source power that would be necessary to make a contribution H_i to the acoustic energy in an infinite uniform medium such that

$$\Delta W_i = 2\alpha c H_i. \tag{5}$$

The average energy density in an enclosure of total volume V_{tot} containing all sources of interest is

$$\langle H_V \rangle = \frac{H_{\text{tot}}}{V_{\text{tot}}}, \tag{6}$$

https://doi.org/10.1121/10.0003960

where the angled brackets indicate a spatial average.

Rearranging Eq. (5) for H_i and substituting in Eq. (1) gives

$$H_{\text{tot}} = \frac{1}{2\alpha c}\sum \Delta W_i. \tag{7}$$

Substituting this result and Eq. (2) in Eq. (6), rearranging for $\langle\overline{p^2}\rangle$, and expressing the result in terms of the spectral density at frequency f gives

$$P \equiv \langle(\overline{p^2})\rangle_f = \frac{\rho c}{2\alpha V_{\text{tot}}}\sum_i \Delta W_{f,i}. \tag{8}$$

A large contribution to ambient sound in the sea is made by sources close to the sea surface, for which it is helpful to think in terms of the sound radiated by a dipole comprising a point monopole source at a (small) depth d and its surface-reflected image. The power radiated by two monopoles in anti-phase depends on the volume velocity of each monopole and the separation between them. Specifically, the element of the power spectral density $\mathrm{d}W_f^{\text{dp}}$ radiated by such a dipole into an annulus of angular width $\mathrm{d}\theta$ (in elevation) into the ocean (represented by a uniform half space) is

$$\mathrm{d}W_f^{\text{dp}} = \frac{8\pi S_f}{\rho c}\sin^2(kd\,\sin\,\theta)\cos\,\theta\,\mathrm{d}\theta, \tag{9}$$

where S_f is the spectral density of the source factor (ISO, 2017) of each monopole source and k is the wavenumber $2\pi f/c$. In the ocean, there exists a (seasonally dependent) critical grazing angle at the sea surface (henceforth, abbreviated "critical surface angle" ψ; see Fig. 2), separating ray paths that interact with the seabed from those that do not.

Sound rays whose grazing angles at the surface are less than this critical surface angle, ψ, are trapped by refraction above the seabed (and by reflection at the sea surface) and, consequently, able to contribute to the global average sound field via the associated waveguide. The equivalent free-field power in this situation is the part of the power radiated by the dipole that is trapped in this waveguide, found by changing the integration variable in Eq. (9) to $u = \sin\theta$ and integrating from $u = 0$ to $u = \sin\psi$

$$\delta W_{f,i} = \frac{4\pi S_{f,i}}{\rho c}[1 - \text{sinc}(2kd_i\,\sin\,\psi)]\sin\,\psi. \tag{10}$$

Ray paths steeper than the critical surface angle are reflected from the seabed and, consequently, experience bottom reflection loss at each cycle. We, therefore, assume the contribution to the integral from angles greater than ψ is negligible.

B. Application to low frequency shipping sound (global average sound model)

Given $S(f)$ and $\alpha(f)$, one can use Eq. (8) [combined with Eq. (10)] to predict the contribution from shipping or other near-surface sound sources to the global average sound budget. At frequencies in the range 200 Hz–10 kHz, the attenuation $\alpha(f)$ in Eq. (8) can be approximated by the contribution due to the boric acid relaxation (Francois and Garrison, 1982; the magnesium sulfate term is unimportant at $f < 10$ kHz),

$$\alpha_{\text{B}}(f) = A_{\text{B}}\frac{f_2}{f_2 + f_{\text{B}}^2}. \tag{11}$$

Below 200 Hz, an additional term of uncertain origin of order 0.3 Np/Mm (2.6 dB/Mm) in magnitude is needed (Kibblewhite and Hampton, 1980). [A similar lower limit is obtained by reasoning that low frequency sound, if not absorbed in the deep ocean, will eventually reach shallow water or land, making it unavailable for the deep water energy partition implied by Eq. (5).] Denoting this additional term α_{min}, the total attenuation coefficient is

$$\alpha(f) = \alpha_{\text{B}}(f) + \alpha_{\text{min}}. \tag{12}$$

Assuming $\delta W_{f,i}$ and $\Delta W_{f,i}$ are equal and substituting for $\delta W_{f,i}$ in Eq. (8) using Eq. (10) gives (assuming incoherent addition of source powers)

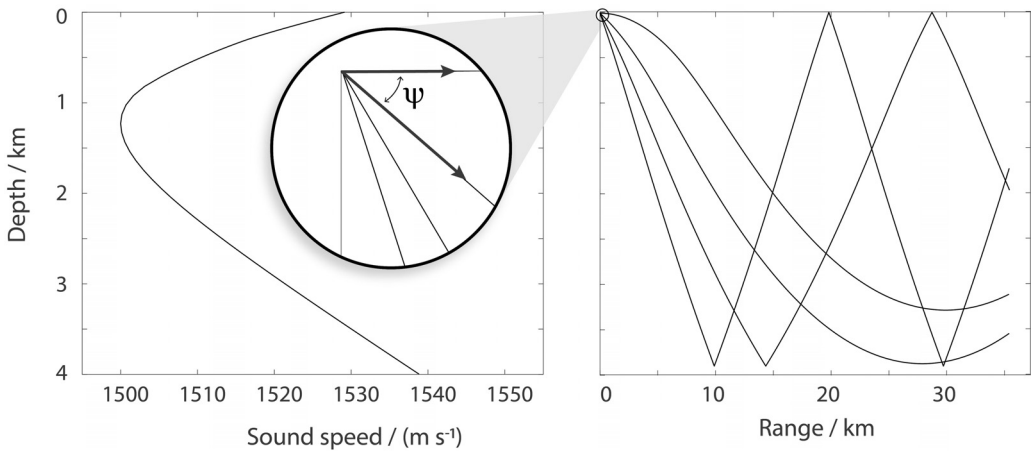

FIG. 2. Illustration of the critical surface angle.

$$P = \frac{2\pi}{V_{\text{tot}}\alpha}\sum_{i=1}^{M} S_{f,i}[1 - \text{sinc}(2kd_i \sin\psi)]\sin\psi \tag{13}$$

or, equivalently,

$$P = 2\pi\frac{M \sin\psi}{V_{\text{tot}}}\frac{\langle S_f(f)\rangle}{\alpha_B(f) + \alpha_{\min}}[1 - \text{sinc}(2kd_{\text{eff}} \sin\psi)], \tag{14}$$

where M is the total number of ships in the region under consideration (an enclosed region of volume V) such that

$$\langle \Delta W_i\rangle = \frac{1}{M}\sum_{i=1}^{M}\Delta W_i, \tag{15}$$

and d_{eff} is an effective monopole depth after averaging, defined as

$$d_{\text{eff}} = \frac{1}{2k \sin\psi}\text{sinc}^{-1}\frac{S_f\langle(f)\text{sinc}\,(2kd \sin\psi)\rangle}{\langle S_f(f)\rangle}. \tag{16}$$

Given estimated values of the number of ships worldwide (M), their mean source factor spectral density $\langle S_f(f)\rangle$, and effective monopole depth (d_{eff}), one can use Eq. (14) to predict the spectral density of the saMSP.

According to Eq. (14), the saMSP depends on the seawater attenuation coefficient but not on the seabed characteristics. This is because the long range sound paths contributing to low frequency ocean sound travel through the ocean at angles close to the horizontal direction and do not interact with the seabed. Steeper paths are stripped away and, hence, do not contribute to the deep ocean sound field as illustrated by Fig. 9 of Farrokhrooz *et al.* (2017), which shows a sharp transition at 17°.

C. Dependence on attenuation coefficient and critical surface angle

Equation (14) shows that saMSP is inversely proportional to the attenuation coefficient (α) as expected from Eq. (4). At high frequency ($2kd_{\text{eff}}\sin\psi \gg 1$) it is proportional to $\sin\psi$, whereas at low frequency ($2kd_{\text{eff}}\sin\psi \ll 1$), Eq. (14) takes the form

$$P = \frac{4\pi M}{3V_{\text{tot}}}\langle S_f(f)\rangle\,(kd_{\text{eff}})^2\frac{\sin^3\psi}{\alpha_B(f) + \alpha_{\min}}, \tag{17}$$

which is proportional to $\sin^3\psi$.

1. Attenuation α: Dependence on bulk properties

The attenuation coefficient α is known to depend on temperature, salinity, and acidity (Francois and Garrison, 1982). According to Joseph and Chiu (2010) and Udovydchenkov *et al.* (2010), the effect of long-term changes in the pH on the ambient sound level is less than 0.01 dB/a, and this is consistent with the application of Eq. (14), which predicts a maximum increase of 1.6 dB at the frequencies of highest sensitivity to pH (below 1000 Hz) for an average drop of 0.2 pH units to 2250. The predicted influence of the changes in salinity and temperature at the sound channel axis is smaller still.

2. Critical surface angle ψ: Dependence on SST

The critical surface angle term, which leads to a dependence on the sound speed at the sea surface c_0 and the seabed c_H, is considered next.

The sound speed is a function of the pressure, temperature, and salinity, all three of which may be approximated, in the absence of mesoscale oceanographic features (e.g., fronts or eddies) as vertically stratified. At the sea surface, the main seasonal dependence arises from changes in the temperature, which means that for the present purpose, ψ can be thought of as a time-dependent function of the SST, $T_0(t)$, i.e., $\psi = \psi(T_0)$.

Defining $\delta c(T_0)$ as the difference in the sound speed between the seabed ($z = H$) and sea surface ($z = 0$) and using Medwin's equation (Medwin, 1975) for the speed of sound in seawater [with practical salinity (Pawlowicz, 2013) $S = 35$] results in

$$\delta c(T_0) = \delta c(0\,^\circ\text{C}) + T_0\left(\text{B} + AT_0 + DT_0^2\right), \tag{18}$$

where

$$\delta c(0\,^\circ\text{C}) = EH - T_H\left(\text{B} + AT_H + DT_H^2\right), \tag{19}$$

and

$$\begin{aligned} A &= 0.055\ \text{m s}^{-1}/^\circ\text{C}^2,\\ \text{B} &= -4.6\ \text{m s}^{-1}/^\circ\text{C},\\ D &= -2.9\times10^{-4}\ \text{m s}^{-1}/^\circ\text{C}^3,\\ E &= 0.016\ \text{m s}^{-1}/\text{m}, \end{aligned} \tag{20}$$

giving the following expression for the critical surface angle as a function of T_0:

$$\begin{aligned} \psi(T_0) &\approx \sqrt{\frac{2\delta c(T_0)}{c_H}}\\ &= \left[2\frac{\delta c(0\,^\circ\text{C}) + T_0\left(\text{B} + AT_0 + DT_0^2\right)}{c_H}\right]^{1/2}. \end{aligned} \tag{21}$$

Equation (21) can be used in combination with Eq. (14) to predict the dependence of the saMSP on the temperature and, therefore, in principle, on season or time of day with a maximum expected when the surface is the coldest (late winter or early morning). Validation of Eq. (14) would require global average sound measurement, which is not presently available. However, the time series of multiple consecutive years are available only from selected deep water stations (Andrew *et al.*, 2011; Prior *et al.*, 2011, 2012; Van der Schaar *et al.*, 2014; Miksis-Olds *et al.*, 2013;

https://doi.org/10.1121/10.0003960

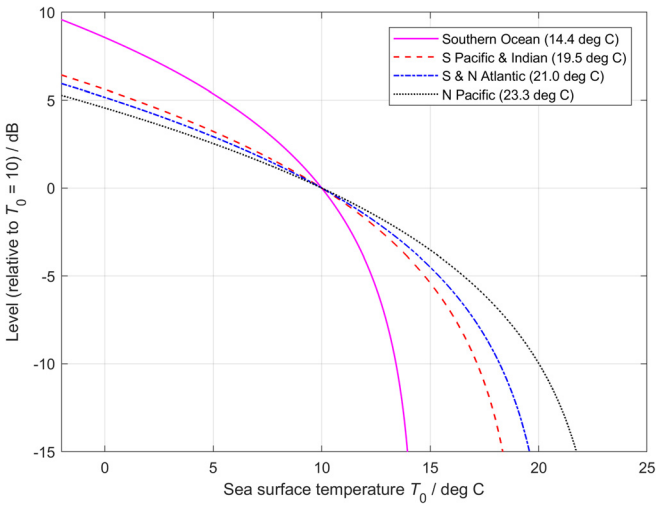

FIG. 3. (Color online) Relative sound level in decibels (relative to the level at $T_0 = 10\,^\circ\mathrm{C}$), calculated as $10\log_{10}[\psi^3(T_0)/\psi^3(10\,^\circ\mathrm{C})]$ using Eq. (22) for the Pacific, Indian, Atlantic, and Southern Oceans with the parameters of Table I. The legend includes, in parentheses, the critical sea surface temperature (CSST) T_c of each ocean, averaged as appropriate.

Miksis-Olds and Nichols, 2016; Harris *et al.*, 2019). A possible compromise until a more comprehensive network can be established is to estimate the seasonal or diurnal dependence of the measured sound level for an ocean basin and compare with the measurements averaged over the available stations in that basin.

Normalizing Eq. (17) relative to $T_0 = 0\,^\circ\mathrm{C}$, the low frequency saMSP is proportional to the ratio

$$\frac{\psi^3(T_0)}{\psi^3(0\,^\circ\mathrm{C})} = \left[1 + \frac{T_0\left(\mathrm{B} + AT_0 + DT_0^2\right)}{\delta c(0\,^\circ\mathrm{C})}\right]^{3/2}. \tag{22}$$

The temperature at depth 3000 m (or greater) can be thought of as approximately constant in each major ocean, equal to 2.5 °C–3.0 °C in the Atlantic Ocean, 0 °C in the Southern Ocean, and 1.5 °C in other oceans, including the Pacific Ocean (Ainslie, 2010, Fig. 4.2). Therefore, within each ocean, the right-hand side of Eq. (22) is a function of T_0 and H only. Figure 3 shows the ratio $\psi^3(T_0)/\psi^3(10\,^\circ\mathrm{C})$ expressed as a level difference in decibels vs T_0 for all of the world's oceans except the Arctic Ocean, calculated using the parameters of Table I.

The form of Eq. (21) is such that the critical surface angle vanishes when some critical sea surface temperature (CSST) T_c, the value of which is determined by the sound speed in water at the seabed, is exceeded. If this happens within some extended geographical region, the contribution to ambient sound outside that region from the surface sound sources within it will be heavily damped because of the absence of a waterborne propagation path from the source to the receiver. For the same reason, if the sources in question are in an enclosed basin, such as the Gulf of Mexico, extreme summer afternoon temperatures in that basin could result in quiet conditions in the entire basin. The world's largest oceans (Pacific, Atlantic, and Indian) have CSSTs between 19 °C and 23 °C (Table I).

III. SUMMARY OF MEASUREMENTS

Measurements of ambient sound for four locations along the North American west coast, covering between them a 12-year period between December 1994 and November 2006, inclusive, are reported by Andrew *et al.* (2011). The four locations (Fig. 4; see also Burtenshaw *et al.*, 2004) are referred to as receivers "*d* (Point Sur)" (Point Sur, CA), "*f* (San Nicolas)" (San Nicolas Island, CA), "*g* (Oregon)" (close to the border between northern California and southern Oregon), and "*h* (Washington)" (close to the border between northern Oregon and southern Washington) with spectra plotted in Fig. 5. The time series of monthly medians in three decidecade bands centered at 16, 80, and 400 Hz are plotted in Fig. 6 and cover a period of approximately 12 years between December 1994 and November 2006. [A decidecade is a logarithmic frequency interval equal to one-tenth of a decade (ISO, 2017). This bandwidth is approximately equal to one-third of an octave and, for this reason, is sometimes referred to as a "one-third octave."] The reason for the use of a median (over multiple snapshots, each of duration 200 s) to represent the monthly average SPL was to approximate the processing used by Wenz (Andrew *et al.*, 2011). The frequencies mentioned

TABLE I. The mean water depth (Costello *et al.*, 2010), temperature at the seabed T_H, and critical sea surface temperature (CSST) of major seas and oceans sorted by CSST T_c, found by solving Eq. (21) with the left-hand side set to zero. Also included is the ocean volume (Costello *et al.*, 2010) to provide an indication of the total size. All seas or oceans whose volume exceeds 5 Mm^3 and mean water depth exceeds 3000 m are included.

Sea or ocean	Mean water depth, H (m)	Temperature at seabed, T_H (°C)	CSST, T_c (°C)	Volume, V (Mm^3)
North Pacific Ocean	4641	1.5	23.3	299.6
Philippine Sea	4347	1.5	21.5	24.8
North Atlantic Ocean	3872	3.0	21.1	132.8
South Atlantic Ocean	3961	2.5	20.8	159.5
Indian Ocean	4036	1.5	19.6	233.4
South Pacific Ocean	3993	1.5	19.4	305.9
Tasman Sea	3369	1.5	16.0	11.3
Arabian Sea	3279	1.5	15.5	13.9
Southern Ocean	3486	0	14.4	70.7

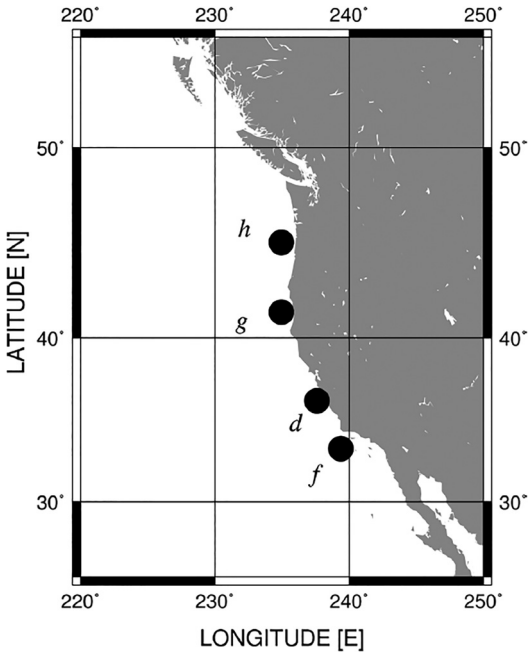

FIG. 4. Location of the four receivers. Reproduced from Andrew *et al.* (2011).

here and throughout are nominal decidecade center frequencies. Precise center frequencies of the decidecade bands are calculated according to IEC (2014).

Hardware anomalies in system *h* resulted in a frequency-dependent upward bias between December 1997 and August 2002. In order to correct for these anomalies, biased measurements were adjusted by a constant value in each decidecade band (Fig. 7). This constant value was determined by equating the mean power spectrum in the time window December 1997–August 2002 to the mean spectrum outside this window.

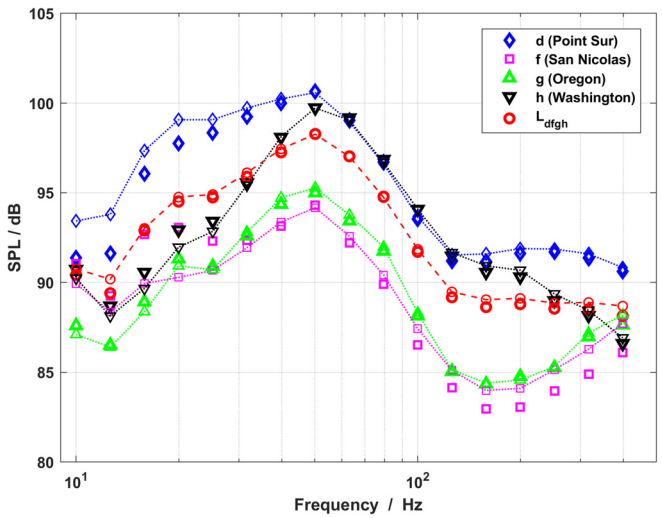

FIG. 5. (Color online) The decidecade band sound pressure level (SPL; re 1 μPa^2) vs the frequency at each of the four receivers, averaged over the 12-year period December 1994–November 2006 (unconnected dark symbols) and the 14-month period May 1998–June 1999 (interconnected pale symbols), and averages (L_{dfgh}) over all four receivers.

Where time is expressed in units of months, the time origin is 1 January 1995 and the definition 1 month $\equiv$ 30.4375 day (one-twelfth of a Julian year) is used. The data available cover the period from 21 November 1994 ($t = -1.3$ months) to 30 November 2006 ($t = 143.0$ months).

There is 1 period of 14 consecutive months from May 1998 to June 1999, inclusive, for which data from all 4 receivers are available. The same 14-month sequence is used to calculate the 4 individual spectra of Fig. 5. Figure 6 shows a time series of monthly median SPLs for three decidecade bands with center frequencies (400, 80, and 16 Hz) chosen to illustrate three qualitatively different temporal patterns for the period of duration 12 years from 1995 to 2006 (left). The red curve in Fig. 6 shows the quantity (L_{dfgh}) for the 14-month sequence,

$$L_{dfgh} = 10 \log_{10} \frac{\frac{1}{4} \sum_{j=d,f,g,h} \left(\overline{p^2}\right)_j}{1\ \mu\text{Pa}^2}\ \text{dB}, \tag{23}$$

where $\left(\overline{p^2}\right)_j$ is the monthly median of the decidecade band MSP at site j. In the frequency range 200–400 Hz, ambient sound in the Northeast Pacific is known to be correlated with wind speed (Curtis *et al.*, 1999). An irregular pattern of maxima during the winter season—peaking around January or February in 1997, 1999, and 2001–2006—is apparent in this frequency range, represented by the 400 Hz band (Fig. 6, upper graphs). This pattern is attributed to wind-driven sound with the main peaks presumably associated with winter storms.

For the bands centered at frequencies 63–125 Hz, represented by the 80 Hz band (Fig. 6, middle graphs), the time series is also characterized by a winter maximum. For these intermediate bands, the pattern is more regular with a maximum close to March each year, correlated with temperature changes. The spatial average is dominated by contributions from receivers d and h because the sound pressure level (SPL) at receivers f and g is about 5 dB lower. Similar annual cycles are reported at Wake Island (Van der Schaar *et al.*, 2014; decidecade centered at 63 Hz; Miksis-Olds and Nichols (2016); 5–115 Hz) and Cape Leeuwin (Harris *et al.*, 2019; 5–105 Hz).

Andrew and co-workers attributed sound in the bands centered at 80 Hz and above to wind (Andrew *et al.*, 2011), but the regular temporal pattern suggests a common origin from 63 to 125 Hz (Fig. 8). The correlation of the SST with the well-known seasonal variation of distant shipping sounds (Andrew *et al.*, 2011) is consistent with the assumption that the main contribution to the North Pacific soundscape in this frequency range comes from distant shipping [see Sec. II A for Eq. (10) and the preceding text, Ainslie, 2012, and Ainslie, 2013).

The 16–32 Hz bands (represented here by the 16 Hz band) exhibit a seasonal pattern with a broad maximum in autumn visible either at d or f in most years during the period 1995–2006. This broad maximum is clearly visible during the period August–November 1998 in the

https://doi.org/10.1121/10.0003960

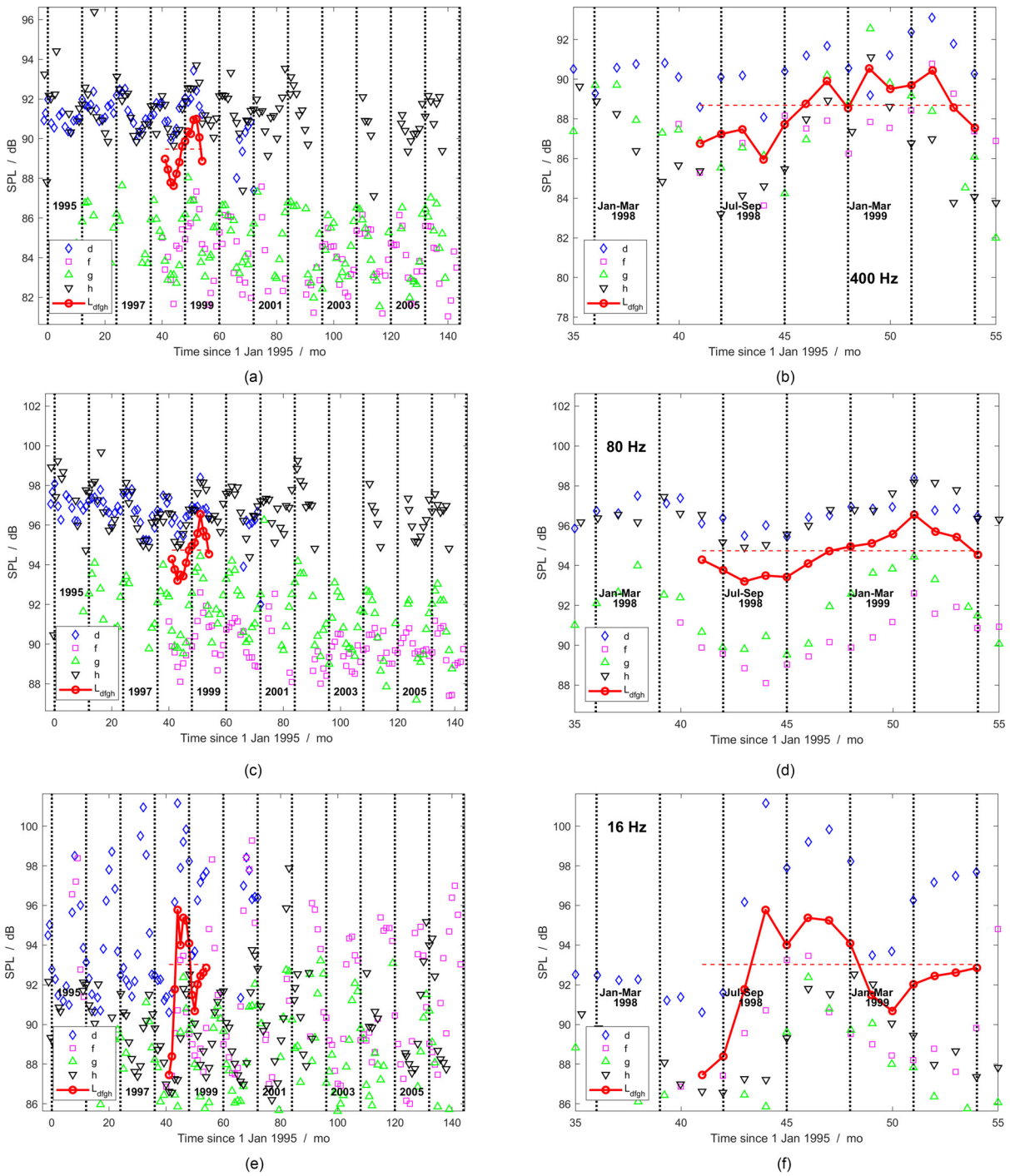

FIG. 6. (Color online) The time series of the monthly medians of the decidecade band SPL (re 1 μPa^2) for each of the four receivers d, f, g, and h vs time in each of three decidecades at nominal center frequencies 400 Hz (upper graphs), 80 Hz (middle), and 16 Hz (lower); the red curves are averaged over all four receivers using Eq. (23) (L_{dfgh}). (Left) 12 years from December 1994 to November 2006, inclusive; (right) 14 months from May 1998 to June 1999, inclusive. The purpose of zooming into the 20-month window (right-hand graphs) is to contrast the regular seasonal pattern at 80 Hz with the more irregular patterns at 16 Hz (likely associated with baleen whale calls) and 400 Hz (winter storms).

four-receiver average but is absent from receiver f (or at least weaker than in other years) in 2001, a year in which there are no data for receiver d. McDonald *et al.* (1995), Curtis *et al.* (1999), Burtenshaw *et al.* (2004); McDonald *et al.* (2006), and Gavrilov *et al.* (2012) associate this frequency range with baleen (fin and blue) whales.

In conclusion, distant shipping dominates the monthly averaged soundscape (at the locations considered here) in decidecade bands with center frequencies between 63 and 125 Hz, being exceeded by baleen whale vocalizations at lower frequencies (up to 32 Hz) and wind-driven sound at higher frequencies (down to 200 Hz). These considerations

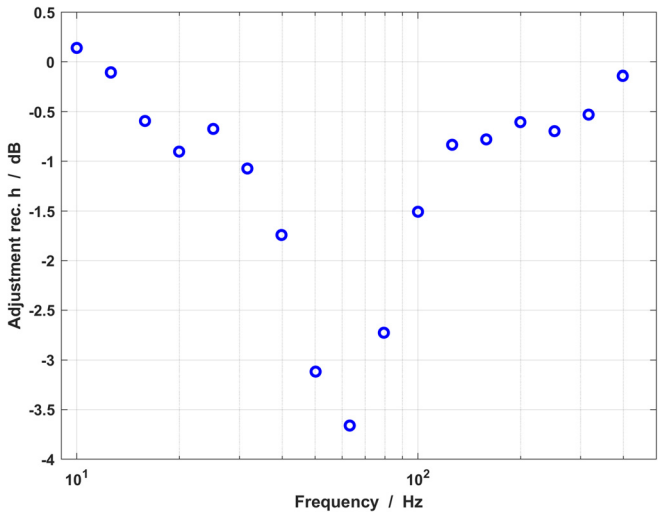

FIG. 7. (Color online) The adjustment added to correct the bias in receiver *h* (Washington) output between December 1997 and August 2002, inclusive.

lead to three distinct frequency bands with monthly aggregates dominated by whale vocalizations (up to 32 Hz), wind (200 Hz and above), and ships at intermediate frequencies (63–125 Hz) with transitions from whale sounds to shipping and from shipping to wind around 40–50 Hz and 160 Hz, respectively. Sites d and f show harmonics of 16 Hz baleen whale calls up to about 100 Hz (see Fig. 3 of Andrew *et al.*, 2011).

This attribution of sources to specific frequency bands differs from that of Andrew *et al.* (2011), which associates the 25–50 Hz decidecade frequency bands with shipping traffic. In the following, the frequency bands centered at 63–125 Hz are compared with theoretical predictions of shipping sound in the same bands.

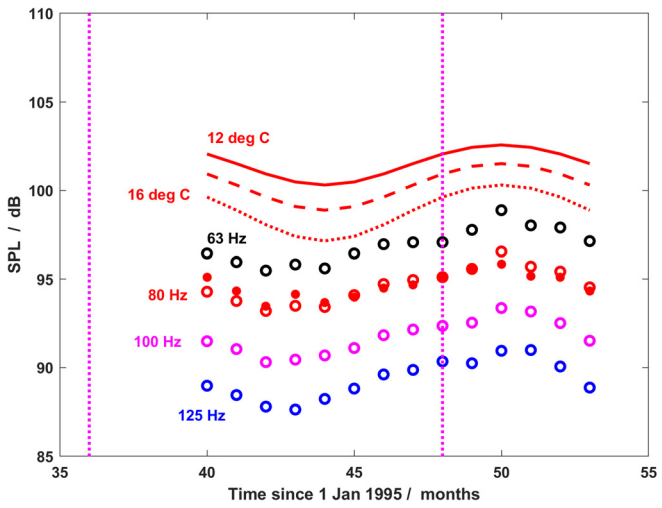

FIG. 8. (Color online) The spatially averaged SPL (re 1 μPa^2) in the decidecade bands from May 1998 to June 1999 centered at 63, 80, 100, and 125 Hz [open circles show measurements averaged over the four receivers (L_{dfgh}) for the 14-month window in 1997–1998 using Eq. (23); filled circles (80 Hz only) are additionally averaged over multiple years; curves show the theoretical prediction of Eq. (14) for a frequency of 80 Hz and the three temperatures 12 °C, 14 °C, and 16 °C]. Vertical dotted lines indicate the start and end of 1998.

Also, relevant are Wenz's 1960s measurements as reported by Andrew *et al.* (2002). These are 3–12 dB lower, depending on the frequency and location, than the 1990s measurements reported by Andrew *et al.* (2002), suggesting an increase of between 0.1 and 0.4 dB/a on average. Despite a steady increase in the number of ships (Fig. 1) and multiple studies aimed at identifying long-term trends (Andrew *et al.*, 2011; Miksis-Olds *et al.*, 2013; Van der Schaar *et al.*, 2014; Miksis-Olds and Nichols, 2016; Harris *et al.*, 2019), the present authors are unaware of evidence that a similar increase has continued into the 21st century. One study (Harris *et al.*, 2019) identified a downward trend in the Southern Ocean.

IV. SOURCE AND MEDIUM PROPERTIES

In this section, the assumed properties of the sound sources (surface vessels) and propagation medium (ocean water) are presented. These properties are used for the predictions of Sec. V.

A. Source properties

Both the total number of ships in the world fleet and the average volume per ship increased nearly threefold between 1964 and 2017 (Table II). This increase in volume implies that the source depth increased by about 45% (Sec. IV A 1). Also needed is the average source factor $\langle S_f(f) \rangle$. As we have no information concerning possible temporal variation in this parameter, we treat it as constant, independent of time between 1964 and 2017 (Sec. IV A 2).

1. Effective source depth (d_{eff})

To apply Eq. (14), we need an estimate of d_{eff} as a function of known parameters, such as gross tonnage, g, which is related to ship volume, V_{ship} (the volume of all enclosed spaces of the ship) according to (International Convention on Tonnage Measurement of Ships, 1969)

$$g = \frac{V_{\text{ship}}}{1\ \text{m}^3}\left(0.2 + 0.02\ \log_{10}\frac{V_{\text{ship}}}{1\ \text{m}^3}\right). \tag{24}$$

The 1964 and 2017 values of the source depth are calculated by assuming that d_{eff} is proportional to $V_{\text{ship}}^{1/3}$ with the 1998 value fixed at the arbitrarily chosen value of 5 m.

2. Source factor spectrum (S_f)

The source factor used is based on Wales and Heitmeyer (2002), abbreviated WH02, which describes measurements of the monopole source level, averaged over 272 merchant vessels in the Mediterranean Sea and Eastern Atlantic Ocean between 1986 and 1992. The reported formula for the mean source spectral density level, $\langle L_{S,f} \rangle$, is

$$\langle L_{S,f} \rangle = 230\ \text{dB} - 35.94\ \log_{10}\frac{f}{1\ \text{Hz}}\ \text{dB} + 9.17\ \log_{10}\left[1 + \left(\frac{f}{340\ \text{Hz}}\right)^2\right]\ \text{dB}. \tag{25}$$

https://doi.org/10.1121/10.0003960

TABLE II. Shipping parameter values used for Fig. 9. The 1998 values of M and d_{eff} are also used for Fig. 10.

Parameter	1964 value	1998 value	2017 value
Total number of vessels (Fig. 1), M	40 380	85 620	115 760
Increase in level attributed to increasing fleet size [Eq. (14)] $10\log_{10}\frac{M}{M_{1964}}$ dB	0.0 dB	3.3 dB	4.6 dB
Total gross tonnage [Hildebrand, 2009; Shipbuilders' Association of Japan (2019), G	150×10^6	530×10^6	1290×10^6
Average gross tonnage per ship, $g=G/M$	3710	6190	11 140
Average ship volume, V_{ship} [see Eq. (24)]	13 200 m^3	21 600 m^3	38 200 m^3
Effective monopole source depth, d_{eff}	4.24 m	5.00 m	6.05 m
Increase in level attributed to increasing ship volume $10\log_{10}\frac{d_{\text{eff}}^2}{(d_{\text{eff}}^2)_{1964}}$ dB	0.0 dB	1.4 dB	3.1 dB
Total expected increase since 1964	0.0 dB	4.7 dB	7.7 dB

To use WH02 data, it is necessary to convert from the reported mean value of the source level to the mean source factor needed in Eq. (14). The spectral density S_f of the source factor of a single vessel is related to the source spectral density level $L_{S,f}$ according to

$$L_{S,f} \equiv 10\log_{10}\frac{S_f(f)}{1\ \mu\text{Pa}^2\,\text{m}^2/\text{Hz}}\ \text{dB}. \tag{26}$$

If, following WH02, the source level follows a normal distribution with mean $\langle L_{S,f}\rangle$ and standard deviation σ, the source factor is log-normally distributed and, therefore (Johnson *et al.*, 1994; Sertlek *et al.*, 2019),

$$10\log_{10}\frac{\langle S_f(f)\rangle}{1\ \mu\text{Pa}^2\,\text{m}^2/\text{Hz}}\ \text{dB} = \langle L_{S,f}\rangle + \frac{(\sigma/\text{dB})^2}{20\log_{10}\text{e}}\ \text{dB}. \tag{27}$$

The value of σ (obtained from Fig. 6 of WH02) depends on the frequency and is set to 5.3 dB for frequencies below 150 Hz and 3.1 dB for frequencies above 400 Hz, decreasing linearly with increasing frequency in between. With these values, the resulting correction term proportional to σ^2 is between 0.5 and 1.4 dB. The term $\langle S_f\rangle$ in Eq. (14) is calculated from Eq. (27), using Eq. (25) for $\langle L_{S,f}\rangle$.

B. Medium properties

The total volume of all oceans combined is estimated to be $V_{\text{tot}} = 1.33\ \text{Mm}^3$ (Charette and Smith, 2010; Costello *et al.*, 2010). The SST in the Northeast Pacific is estimated to be $T_0 = 14\,^\circ\text{C}$ (Yashayaev and Zveryaev, 2001), the average of the range 12 °C–16 °C.

The minimum low frequency attenuation in the North Pacific is estimated to be $\alpha_{\text{min}} = 0.3$ Np/Mm (2.6 dB/Mm; Kibblewhite and Hampton, 1980, Fig. 6), the average of the range 0.2–0.4 Np/Mm.

Ocean acidity is characterized by the pH parameter K, introduced by Mellen *et al.* (1987), and is related to the pH according to

$$K = 10^{\text{pH}_{\text{NBS}}-8}. \tag{28}$$

A value of $K = 0.6$ is used (Ainslie, 2010, Fig. 4.14), corresponding to $\text{pH}_{\text{NBS}} = 7.78$ ($\text{pH}_{\text{SWS}} = 7.63$).

In the context of trends over multiple decades, all medium properties, including the SST, are assumed to be unchanged during the period 1964–2017. Seasonal fluctuations in the SST are considered in Sec. V C.

V. COMPARISON BETWEEN THEORY AND MEASUREMENT

In this section, the measurements of Sec. III are compared with theoretical predictions made using Eq. (14) and the source and medium properties specified in Sec. IV.

A. Point Sur, CA (1963–1965 and 1994–2001): Spectra

Measurements at Point Sur (receiver d) exhibit an increase of 3–11 dB in the sound level from the 1960s to the end of the 20th century (Andrew *et al.*, 2011). Figure 9 shows the SPL measured by Wenz (1969) at Point Sur between 1963 and 1965 (circles) and Andrew and coworkers between 1994 and 2001 (squares) as reported by Andrew *et al.* (2002). The largest increases in the level occurred in the decidecades centered at 32 and 40 Hz. The

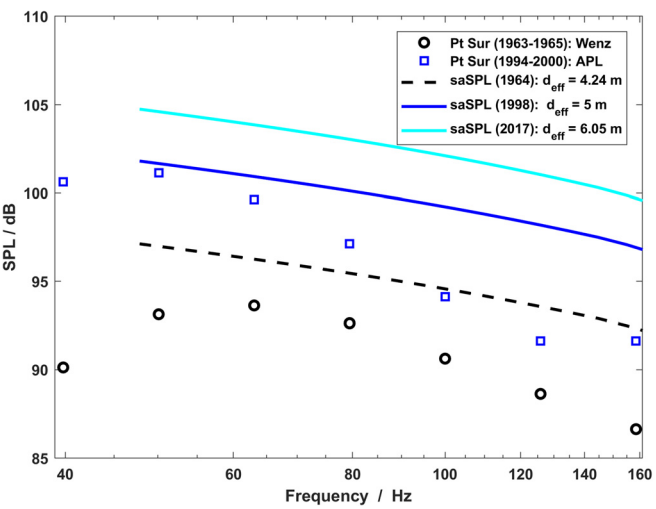

FIG. 9. (Color online) The measured and predicted SPLs (re $1\mu\text{Pa}^2$) vs the frequency. Measurements are for Point Sur (receiver d) from Andrew *et al.* (2002) for 1963–1965 (circles) and 1994–2001 (squares). Predictions are saSPL for 1964 (dashed), 1998 (solid, dark), and 2017 (solid, light). $T_0 = 14\,^\circ\text{C}$; $\alpha_{\text{min}} = 0.3$ Np/Mm (2.6 dB/Mm).

level in the one-fifth decade frequency band comprising these two decidecades, calculated from Table II in Andrew *et al.* (2011), increased from 92.6 dB re 1 μPa^2 in 1963–1965 to 102.3 dB re 1 μPa^2 in 1994–2007. The 32 Hz band is associated with blue whale vocalizations (Burtenshaw *et al.*, 2004; McDonald *et al.*, 2006).

Also shown in Fig. 9 (40–160 Hz bands, of which 63–125 Hz are the bands of interest) are theoretical predictions using Eq. (14) for the years 1964, 1998, and 2017 with the parameters of Table II. The predicted increase from 1964 to 1998 in the frequency range 63–125 Hz is 4.7 dB, similar to the observed change in that frequency range (Fig. 9). The predicted increase from 1964 to 2017 in the same frequency range is 7.7 dB. Absolute levels are not directly comparable because the measurement is for a single site, whereas the prediction is for a spatial average. The measurements of Chapman and Price (2011), made in 1978 and 1980 at a different site in the Northeast Pacific, show an increase relative to Wenz's 1965 measurements at Point Sur of about 3 dB in the 63–125 Hz bands.

B. Northeast Pacific Ocean (1997–1999): Spectra and sensitivity

To compare any measurement with Eq. (14), a spatial average is needed. In principle, this spatial average should be for an entire ocean basin. In practice, we make do with the four receivers available, recognizing that in the absence of a basin scale measurement network, the presently available data set is necessarily incomplete.

The use of Eq. (14) is also subject to uncertainty in some of its input parameters, especially in the low frequency absorption coefficient $\alpha_{\min}$ and the SST (T_0, a proxy for the critical angle, ψ). Sensitivity to these two parameters is considered next (Fig. 10).

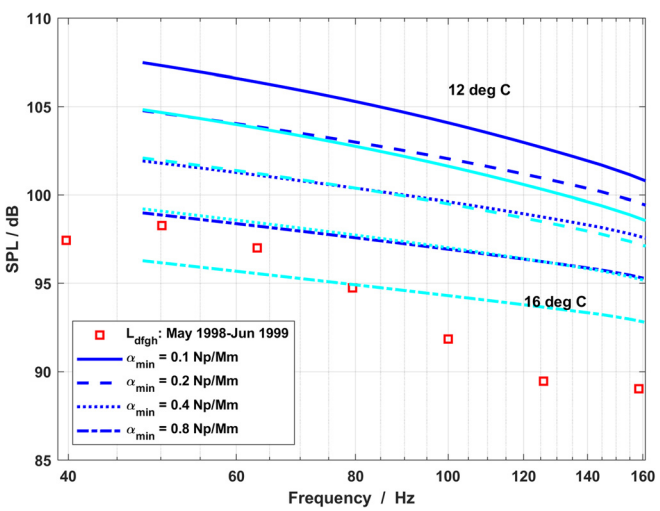

FIG. 10. (Color online) Sensitivity of the spatially averaged decidecade band shipping SPL (re 1 μPa^2) spectrum to the SST T_0 (12 °C = dark and 16 °C = light) and low frequency attenuation $\alpha_{\min}$ (0.1–0.8 Np/Mm) calculated using the Wales-Heitmeyer source spectrum for monopole source depth $d_{\text{eff}} = 5.0$ m. The squares indicate the May 1998–June 1999 L_{dfgh} measurements in the frequency range 40–160 Hz (from Fig. 5).

Our predictions are for the saMSP, the measurement of which would require a large global grid of receivers in latitude, longitude, and depth. Even if one's ambition is limited to an average over (say) the North Pacific Ocean, the required number of receivers is much greater than four. It is, therefore, likely that an estimate of the spatially averaged sound pressure level (saSPL) based on only the four stations (L_{dfgh}) is biased, but we are unable to say in which direction. All four receivers are at remote locations along the US Pacific coast, and all are in the deep sound channel [ideally, one would sample at multiple depths, including maxima at the sea surface and the conjugate depth and minimum below the conjugate depth (Weston, 1980; Farrokhrooz *et al.*, 2017]. Further, the global average is based on the MSP, which is expected to exceed the median (used by Andrew *et al.*, 2011) by an amount that depends on the fluctuations about the mean (Van der Graaf *et al.*, 2012; Merchant *et al.*, 2012; Dekeling *et al.*, 2014; Van der Schaar *et al.*, 2014); the median processing presently used (Andrew *et al.*, 2011) could be replaced with the arithmetic mean (MSP) to provide an average more directly comparable with the prediction. The difference between mean and median measured at four deep ocean sites is between 0.2 and 1.6 dB (Dekeling *et al.*, 2014, p. 51) at 63 Hz. It is also possible that the theoretical prediction is biased due to the simplifying assumptions made in its derivation. In the following, we consider simplifications to the source model and the propagation model.

- First, we consider the source model. In the spirit of Ockham's razor, we have applied the simplest source level model compatible with available facts by using the WH02 spectrum for all ships from 1964 to 1998. The source depth is assumed to be proportional to other linear dimensions of a ship, which, in turn, are assumed to be proportional to the cube root of the average ship volume. The calculations assume all ships are at sea all of the time, which is likely to overestimate the average. On the other hand, sources other than shipping (e.g., geophysical sources, biota, or other man-made sources such as airgun arrays), while expected to be minor in the 63–125 Hz bands, must nevertheless contribute to the total sound field.
- The propagation model developed in Sec. II makes a number of simplifying assumptions requiring the water depth, SST, and attenuation coefficient to be uniform and independent of geographical position. In reality, the water depth varies between zero at the coastline and more than 10 km in the deepest trenches. Many of the shipping lanes are in relatively shallow water and as a result contribute less to the deep water sound field than the same ships would have contributed in (cold) deep water. The sound radiated by ships in shallow water is attenuated by multiple seabed reflections before reaching the continental slope and deep ocean. Whereas ignoring this attenuation mechanism might overestimate the low frequency saMSP, the contribution from ships close to or on the continental

https://doi.org/10.1121/10.0003960

slope might then be underestimated by not considering the downslope conversion (Wales and Diachok, 1981; Dashen and Munk, 1984; Carey *et al.*, 2009). The geographical dependence of pH (Mellen *et al.*, 1987) will result in corresponding variations in the attenuation coefficient, but this effect seems minor compared with the bathymetry and SST variations. Finally, the choice of 14 °C and 0.3 Np/Mm might bias the estimate of the attenuation at high and low frequencies, respectively.

A complete explanation of the 5 dB discrepancy (the difference between saSPL and L_{dfgh} in Fig. 8) is most likely a combination of more than one of the above factors, but the proximity of major shipping lanes to land makes it probable that at any one time, many of the sources are in shallow water (including some in ports or anchored). Use of known water depth and SST distributions, combined with a realistic shipping distribution based on known shipping traffic, is expected to result in improved predictions of the saMSP.

A second discrepancy arises in the vertical angle dependence of the sound field. The proposed range-independent model would result in a distinctive distribution of elevation angles with a null in the horizontal direction and a peak at an angle equal to $\operatorname{acos}\left[c(z)/c(0)\right]$, varying with the receiver depth z according to Snell's law. While the expected peak has been observed (Wales and Diachok, 1981), the null is filled in (Wales and Diachok, 1981; Farrokhrooz *et al.*, 2017), indicating important contributions from paths not predicted by the simple model. Wales and Diachok (1981) suggest one possible mechanism involving the downslope conversion from surface vessels on or near the continental slope (Dashen and Munk, 1984). The horizontal null can be filled in for geometries involving downslope propagation (Carey *et al.*, 2009).

Bannister (1986) suggests a seasonal contribution at 50 Hz from distant "wind-noise lanes." The levels he predicts for this mechanism are about 10 dB lower and of larger amplitude (ca. 3.5 dB cf 1.2 dB) than the seasonal patterns we attribute to distant shipping. However, the same mechanism applies to sound from surface vessels in a surface channel at high latitude, which would couple in the same way into the deep sound channel at moderate latitude, similar to the mechanism suggested by Bannister for wind, thus, providing an alternative mechanism to fill in the null.

C. Northeast Pacific Ocean: Annual cycle

An annual cycle in ambient sound can be expected due to seasonal changes in the SST with maximum levels expected in late winter when the SST is at a minimum (Ainslie, 2012). Annual cycles in the northern Pacific Ocean have been reported by Andrew *et al.* (2011) (US west coast, 25–50 Hz) and Van der Schaar *et al.* (2014) (Wake Island, 63 Hz), both with a pronounced maximum in winter and an amplitude (half of the total spread) of ca. 2 dB. A winter maximum at the (lower) frequencies associated with wind sound (200–500 Hz) can be attributed to storms, but a winter maximum at frequencies dominated by shipping suggests a different explanation is required. The possibility that this maximum is caused by seasonal fluctuations in the SST is considered next.

Measurements of the SST averaged in monthly intervals over the southern North Pacific Ocean (latitude up to ~30° N) between 1998 and 2010. Signorini and McClain (2012) exhibit seasonal fluctuations of amplitude $T_A = 1.7$ °C about a mean of about $\bar{T} = 25.5$ °C. The receivers considered in the present paper (Fig. 4) are all in the Northeast Pacific where the mean temperature is lower (12 °C–16 °C) and the amplitude is about 2 °C (Yashayaev and Zveryaev, 2001). The main shipping lanes are further north, where the mean temperature is lower still (between 7 °C at 50° N and 14 °C at 40° N) and the amplitude of the seasonal SST fluctuations is higher (about 4 °C; Yashayaev and Zveryaev, 2001). In the following, we base the predictions on temperature variations of the form

$$T_0(t) = \bar{T} + T_A \sin\left(\frac{2\pi}{\tau}(t - 5\ \text{month})\right), \tag{29}$$

where τ is the period, equal to 12 months, T_A is the amplitude, and the 5-month phase shift implies a surface temperature minimum in early March, 2 months (about 61 days) after the start of each year (Yashayaev and Zveryaev, 2001). The time origin is 1 January.

The critical surface angle that follows from the temperature variation [Eq. (21)] is substituted in Eq. (14) to calculate the theoretical seasonal variation in the sound level. Figure 8 shows L_{dfgh} in four decidecade bands (63–125 Hz), plotted vs time during the period December 1997–June 1999. The symbols show measurements averaged over the four receivers using Eq. (23) to facilitate the comparison between prediction (curves) and measurement (symbols). Whereas the predictions exceed the measurements by 5 dB (Fig. 8), apart from some noise close to the minimum, the amplitude and phase of the seasonal fluctuations are accurately estimated. Notice that the minimum predicted at $t = 43$ months, corresponding to the temperature maximum (minimum critical surface angle) in late summer, and coinciding with a minimum in the measured sound level. The 2 °C amplitude of the temperature oscillations translates to an amplitude of 1.2 dB in level fluctuations, implying a sensitivity of -0.6 dB/°C.

D. Implications of SST-driven cycle

The hypothesized explanation for seasonal fluctuations in the saMSP in terms of seasonal fluctuations in SST implies that the saMSP changes with the SST at a rate determined by the sensitivity of the critical surface angle ψ to the SST

$$\frac{\mathrm{d}\psi}{\mathrm{d}T_0} = -\frac{1}{c_0 \tan\psi}\frac{\mathrm{d}c_0}{\mathrm{d}T_0}. \tag{30}$$

The sensitivity of the saMSP to the SST,

$$\frac{dP}{dT_0} = \frac{dP}{d\psi}\frac{d\psi}{dT_0}, \tag{31}$$

is, therefore (limiting attention to low frequency),

$$\frac{dP}{dT_0} = -\frac{3P/c_0}{\tan^2\psi}\frac{dc_0}{dT_0}. \tag{32}$$

Finally, the sensitivity of the saSPL (the level of the saMSP) to the SST,

$$\frac{dL}{dT_0} = \frac{dL}{dP}\frac{dP}{dT_0}, \tag{33}$$

is

$$\frac{dL}{dT_0} = -\frac{30\ \log_{10}e}{c_0\tan^2\psi}\frac{dc_0}{dT_0}\ \text{dB}. \tag{34}$$

Using $\psi = 0.20$ and $dc/dT = 3.2\,(\text{m s}^{-1})/^\circ\text{C}$ (Medwin, 1975), corresponding to $T_0 = 14\,^\circ\text{C}$, practical salinity $S = 35$, and depth $z = 0$, we obtain

$$\frac{dL}{dT_0} = -0.66\,\frac{\text{dB}}{^\circ\text{C}}, \tag{35}$$

which compares with the measured value for this quantity of -0.6 dB/°C [see the discussion following Eq. (29)].

VI. SUMMARY AND DISCUSSION

We have analyzed 16–400 Hz decidecade band measurements of monthly averaged SPLs vs time at four sites in the Northeast Pacific Ocean from December 1994 to November 2006. We find the bands with center frequencies between 63 and 125 Hz best suited for studying ambient sound contributions from distant vessels. At higher frequencies (160–400 Hz bands), the shipping signal is contaminated by wind. Lower frequencies (16–32 Hz) contain information about the vocalizations of baleen whales. The 40 and 50 Hz bands are likely to contain contributions from shipping and baleen whales.

A. 63–125 Hz

1. Theoretical model (shipping)

We present a theoretical model for the shipping contribution to the saMSP (symbol P). The result is proportional to the number of ships per unit volume of ocean and the average source factor ($\langle S\rangle$) and inversely proportional to the seawater attenuation coefficient. It also depends on the total gross tonnage (G), the gross tonnage per ship (g), and the critical surface angle (ψ) in a manner that depends on the frequency. McDonald *et al.* (2006) suggested that the shipping contribution to the MSP might be proportional to G ($10\log_{10}G$ dB), whereas Frisk (2012) assumed proportionality to G^2 ($20\log_{10}G$ dB). Assuming $d \sim g^{1/3}$, Eq. (17) predicts the proportionality of P to $\langle S\rangle G g^{-1/3}\sin^3\psi$ at low frequency, roughly consistent with the dependence on tonnage as suggested by McDonald (2006).

The model predicts a saSPL (level of saMSP) of 100 dB in 1998 in the 80 Hz decidecade band in the Northeast Pacific Ocean (Fig. 8), about 5 dB higher than the observed value, L_{dfgh} (averaged over four sites) of 95 dB (Figs. 8 and 10). Possible contributors to the 5 dB discrepancy are listed in Sec. V B. Of these, we highlight a bias in the prediction caused by overestimating the number of ocean-going vessels (the theoretical prediction assumes, unrealistically, that all ships are in deep water all of the time) and partly to a 0.2–1.6 dB bias in the measurement caused by use of a monthly median instead of the arithmetic mean.

2. Seasonal fluctuations

The model predicts seasonal fluctuations in P because ψ is a function of the SST. A maximum is predicted in early March when the SST is lowest and an amplitude (of level fluctuations) of 1.3 dB at 80 Hz in the Northeast Pacific Ocean compared with an observed amplitude of 1.2 dB (maximum also in March), implying a sensitivity of 0.6 dB/°C.

Because sensitivity to temperature is approximately inversely proportional to $\tan^2\psi$ [Eq. (34)], the seasonal fluctuations might be more noticeable in regions with either a higher SST or lower CSST or both such as the Indian Ocean (Wang *et al.*, 2019). For example a reduction in ψ by a factor two (to 0.1) increases the sensitivity to temperature by a factor 4 (to 2.4 dB/°C).

3. Long-term changes: 1964–1998

The predicted increase in the saSPL due to increased shipping tonnage between 1964 and 1998, assuming no change in the SST, is 4.7 dB. Assuming an increase in the SST from 14.0 °C to 14.7 °C in 34 years (corresponding to 0.02 °C /a; Wu *et al.*, 2011) decreases the predicted increase by 0.4 dB, resulting in a net predicted increase of 4.3 dB, compared with a measured increase at Point Sur (receiver d) in the shipping bands (63–125 Hz) of 3–6 dB (Fig. 11).

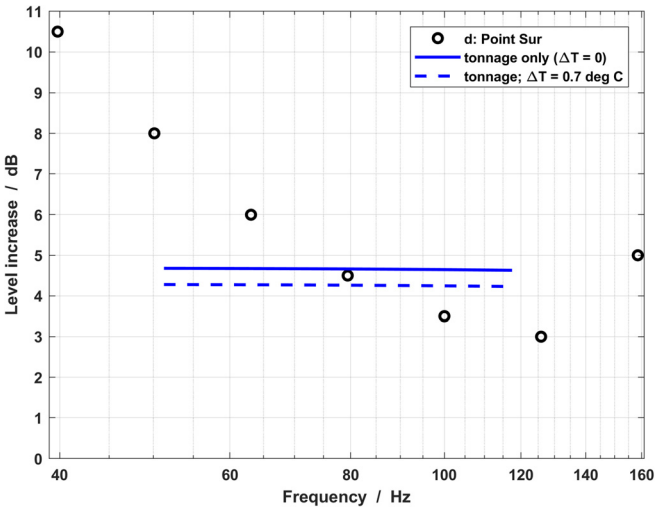

FIG. 11. (Color online) The increase in the level from 1964 to 1998. Symbols denote the measured increase at receiver d (Point Sur; Andrew *et al.*, 2011), the solid line denotes Eq. (14) with $T = 14.0\,^\circ\text{C}$, the dashed line denotes Eq. (14) with an increased temperature of 14.7 °C.

Thus, in this frequency range, the observed increase is fully explained without invoking the increase in the source level considered necessary by McDonald *et al.* (2006). Instead, the unexplained increase of 9–12 dB occurs in the frequency range of baleen whale vocalizations (Sec. VI B).

Taken at face value, the 3 dB increase at 125 Hz (Fig. 11) might seem consistent with the predicted increase from doubling the number of vessels alone. In reality though, the 125 Hz band includes a contribution from wind. If one makes the (arbitrary but plausible) assumption that in 1964 the contributions from wind and shipping were equal in this band, if the wind contribution remained constant, a 3 dB increase in the band would require a threefold (5 dB) increase in the shipping contribution.

4. Long-term changes: 1998–2017

The predicted 1998–2017 increase in the level is approximately 3 dB, but no major study has shown an increase of this magnitude in the 21st century (Andrew *et al.*, 2011; Miksis-Olds *et al.*, 2013; Miksis-Olds and Nichols, 2016; Harris *et al.*, 2019). We do not have an explanation for this discrepancy but consider the following questions worth investigating:

- have changes in ship design or maintenance led to noticeable changes in their draft, source level, or proportion of time spent at sea?
- have changes in shipping distribution led to an increasing proportion of ships in warm or shallow water?
- has gradual long-term warming of the sea surface led to a reduction in the sound detected in the deep ocean from surface ships?
- does the sound in regions where levels are stable or decreasing originate from sources other than surface vessels?

Of these questions, the second and third can usefully be investigated by means of a more detailed modelling approach than used in this paper. Detailed shipping and oceanographic databases exist that could be used alongside long-range propagation modelling methods, including effects of fronts and bathymetry, to investigate whether changing SST or shipping distribution play a role.

B. 16–32 Hz

By attributing the 5 dB increase in the 63–125 Hz bands to a growth in gross tonnage, we have so far left unaddressed the question of what causes the ∼10 dB increase at lower frequencies. Given that the 16–32 Hz bands are associated primarily with blue whale calls (Burtenshaw *et al.*, 2004; McDonald *et al.*, 2006), a plausible explanation involves an increased population, possibly in combination with more vocal individuals, perhaps to counter higher masking noise. The simplest (though highly speculative) explanation is a tenfold increase in the population of blue whales in 30 years, implying a growth rate of $0.077\,a^{-1}$ (115% increase every 10 years). For comparison, a factor 5–10 increase in the abundance in the southern right whale population is estimated by Cooke and Zerbini (2018).

Since the early 1990s, the population has stayed approximately constant at about 2000 individuals (NMFS, 2020), consistent with the absence of an increase in the 16–32 Hz bands since 1994 (Andrew *et al.*, 2011).

VII. CONCLUSIONS

A. Shipping bands: 63–125 Hz

The 63–125 Hz bands are dominated by contributions from shipping. In this frequency range, the globally averaged MSP is proportional to $Gg^{-1/3}\sin^3\psi$. The observed 5 dB increase from 1964 to 1998 in these bands can be explained by changes in M and g alone with no change in the source level. Seasonal fluctuations in these bands can be explained by changes in the SST alone.

B. Baleen whale vocalization bands: 16–32 Hz

The observed ∼10 dB increase from 1964 to 1998 occurs primarily in the 16–32 Hz bands, which are dominated by contributions from baleen whale vocalizations.

C. Transition bands: 40–50 Hz

The intermediate frequency (40–50 Hz) bands include contributions from shipping in the winter and baleen whale calls in the summer. Further work would be required to separate these contributions.

Ainslie, M. A., De Jong, C. A. F., Dol, H. S., Blacquière, G., and Marasini, C. (**2009**). "Assessment of natural and anthropogenic sound sources and acoustic propagation in the North Sea," TNO report DV2009 C085 (TNO, Den Haag), p. 64, available at https://publications.tno.nl/publication/34618532/Zby01E/TNO-DV2009C085.pdf (Last viewed 2021-01-17).

Ainslie, M. A. (**2010**). *Principles of Sonar Performance Modeling* (Springer-Praxis, Chichester), pp. 60, 96, 575, 608.

Ainslie, M. A. (**2012**). "Potential causes of increasing low frequency ocean noise levels," Proc. Mtgs. Acoust. **12**(1), 070004.

Ainslie, M. A. (**2013**). "Periodic changes in ambient noise: Possible causes and implications for long term prediction," in *Proceedings of 1st International Conference on Underwater Acoustics*, 23–28 June 2013, Corfu, Greece, pp. 655–662.

Andrew, R. K., Howe, B. M., Mercer, J. A., and Dzieciuch, M. A. (**2002**). "Ocean ambient sound: Comparing the 1960s with the 1990s for a receiver off the Californian coast," ARLO **3**, 65–70.

Andrew, R. K., Howe, B. M., and Mercer, J. A. (**2011**). "Long-time trends in ship traffic noise for four sites off the North American West Coast," J. Acoust. Soc. Am. **129**, 642–651.

Bannister, R. W. (**1986**). "Deep sound channel noise from high-latitude winds," J. Acoust. Soc. Am. **79**, 41–48.

Brewer, P. G., and Hester, K. (**2009**). "Ocean acidification and the increasing transparency of the ocean to low-frequency sound," Oceanography **22**(4), 86–93.

Burtenshaw, J. C., Oleson, E. M., Hildebrand, J. A., McDonald, M. A., Andrew, R. K., Howe, B. M., and Mercer, J. A. (**2004**). "Acoustic and satellite remote sensing of blue whale seasonality and habitat in the Northeast Pacific," Deep Sea Res. Part II: Topical Stud. Oceanogr. **51**(10-11), 967–986.

Carey, W. M., Evans, R. B., Davis, J. A., and Botseas, G. (**2009**). "Deep-ocean vertical noise directionality," IEEE J. Oceanic Eng. **15**, 324–334.

Chapman, N. R., and Price, A. (**2011**). "Low frequency deep ocean ambient noise trend in the Northeast Pacific Ocean," J. Acoust. Soc. Am. **129**, EL161–EL165.

Charette, M. A., and Smith, W. H. (**2010**). "The volume of Earth's ocean," Oceanography **23**(2), 112–114.
Cooke, J. G., and Zerbini, A. N. (**2018**). "*Eubalaena australis*," The IUCN Red List of Threatened Species 2018, e.T8153A50354147, available at https://dx.doi.org/10.2305/IUCN.UK.2018-1.RLTS.T8153A50354147.en (Last viewed 2021-02-03).
Costello, M. J., Cheung, A., and De Hauwere, N. (**2010**). "Surface area and the seabed area, volume, depth, slope, and topographic variation for the world's seas, oceans, and countries," Environ. Sci. Technol. **44**(23), 8821–8828.
Curtis, K. R., Howe, B. M., and Mercer, J. A. (**1999**). "Low-frequency ambient sound in the North Pacific: Long time series observations," J. Acoust. Soc. Am. **106**, 3189–3200.
Dashen, R., and Munk, W. (**1984**). "Three models of global ocean noise," J. Acoust. Soc. Am. **76**, 540–554.
Dekeling, R. P. A., Tasker, M. L., Van der Graaf, A. J., Ainslie, M. A., Andersson, M. H., André, M., Borsani, J. F., Brensing, K., Castellote, M., Cronin, D., Dalen, J., Folegot, T., Leaper, R., Pajala, J., Redman, P., Robinson, S. P., Sigray, P., Sutton, G., Thomsen, F., Werner, S., Wittekind, D., and Young, J. V. (**2014**). "Monitoring Guidance for Underwater Noise in European Seas, Part III: Background Information and Annexes," JRC Scientific and Policy Report EUR 26556 EN (Publications Office of the European Union, Luxembourg).
Farrokhrooz, M., Wage, K. E., Dzieciuch, M. A., and Worcester, P. F. (**2017**). "Vertical line array measurements of ambient noise in the North Pacific," J. Acoust. Soc. Am. **141**, 1571–1581.
Francois, R. E., and Garrison, G. R. (**1982**). "Sound absorption based on ocean measurements. Part II: Boric acid contribution and equation for total absorption," J. Acoust. Soc. Am. **72**, 1879–1890.
Frisk, G. V. (**2012**). "Noiseonomics: The relationship between ambient noise levels in the sea and global economic trends," Sci. Rep. **2**, 1–4.
Gavrilov, A. N., McCauley, R. D., and Gedamke, J. (**2012**). "Steady inter and intra-annual decrease in the vocalization frequency of Antarctic blue whales," J. Acoust. Soc. Am. **131**, 4476–4480.
Harris, P., Sotirakopoulos, K., Robinson, S., Wang, L., and Livina, V. (**2019**). "A statistical method for the evaluation of long term trends in underwater noise measurements," J. Acoust. Soc. Am. **145**, 228–242.
Hester, K. C., Peltzer, E. T., and Brewer, P. G. (**2008**). "Unanticipated consequences of ocean acidification: A noisier ocean at lower pH," Geophys. Res. Lett. **35**, L19601, https://doi.org/10.1029/2008GL034913 .
Hildebrand, J. A. (**2009**). "Anthropogenic and natural sources of ambient noise in the ocean," Mar. Ecol. Prog. Ser. **395**, 5–20.
International Convention on Tonnage Measurement of Ships (**1969**). *Admiralty and Maritime Law Guide*. London, 23 June, available at http://www.admiraltylawguide.com/conven/tonnage1969.html (last viewed 2019-12-28).
IEC. (**2014**). 61260-1:2014, *Electroacoustics—Octave-band and fractional-octave-band filters—Part 1: Specifications* (International Electrotechnical Commission, Geneva).
International Association of Oil and Gas Producers (**2011**). "An overview of marine seismic operations," OGP Report No. 448, International Association of Oil and Gas Producers, available at https://www.norskoljeoggass.no/contentassets/ae812078242441fb88b75ffc46e8f849/an-overview-of-marine-seismic-operations.pdf ((Last viewed 2020-07-05).
ISO. (**2017**). 18405:2017, *Underwater Acoustics—Terminology* (International Organization for Standardization, Geneva).
Johnson, N. L., Kotz, S., and Balakrishnan, N. (**1994**). Continuous univariate distributions, *Volume 1*, 2nd ed. (Wiley, New York), Chap. 14.
Joseph, J. E., and Chiu, C.-S. (**2010**). "A computational assessment of the sensitivity of ambient noise level to ocean acidification," JASA Express Lett. **128**, EL144–EL149.
Kibblewhite, A. C., and Hampton, L. D. (**1980**). "A review of deep ocean sound attenuation data at very low frequencies," J. Acoust. Soc. Am. **67**, 147–157.
McDonald, M. A., Hildebrand, J. A., and Webb, S. C. (**1995**). "Blue and fin whales observed on a seafloor array in the Northeast Pacific," J. Acoust. Soc. Am. **98**, 712–721.
McDonald, M. A., Hildebrand, J. A., and Wiggins, S. M. (**2006**). "Increases in deep ocean ambient noise in the Northeast Pacific west of San Nicolas Island, California," J. Acoust. Soc. Am. **120**, 711–718.
McDonald, M. A., Hildebrand, J. A., Wiggins, S. M., and Ross, D. (**2008**). "A 50 year comparison of ambient ocean noise near San Clemente Island: A bathymetrically complex coastal region off Southern California," J. Acoust. Soc. Am. **124**, 1985–1992.
Medwin, H. (**1975**). "Speed of sound in water: A simple equation for realistic parameters," J. Acoust. Soc. Am **58**, 1318–1319.
Mellen, R. H., Scheifele, P. M., and Browning, D. G. (**1987**). "Global model for sound absorption in sea water. Part II: Geosecs PH Data Analysis," (TR 7925), p. 6.
Merchant, N. D., Blondel, P., Dakin, D. T., and Dorocicz, J. (**2012**). "Averaging underwater noise levels for environmental assessment of shipping," J. Acoust. Soc. Am. **132**, EL343–EL349.
Miksis-Olds, J. L., and Nichols, S. M. (**2016**). "Is low frequency ocean sound increasing globally?," J. Acoust. Soc. Am. **139**, 501–511.
Miksis-Olds, J. L., Bradley, D. L., and Maggie Niu, X. (**2013**). "Decadal trends in Indian Ocean ambient sound," J. Acoust. Soc. Am. **134**, 3464–3475.
National Marine Fisheries Service (**2020**). "BLUE WHALE (*Balaenoptera musculus musculus*): Eastern North Pacific Stock," available at https://www.fisheries.noaa.gov/national/marine-mammal-protection/marine-mammal-stock-assessment-reports-species-stock#cetaceans—large-whales (Last viewed 2021-01-17).
Pawlowicz, R. (**2013**). "Key physical variables in the ocean: Temperature, salinity, and density," Nat. Educ. Knowl. **4**(4), 1–7.
Pierce, A. D. (**1989**). *Acoustics: An Introduction to Its Physical Principles and Applications* (American Institute of Physics, New York), p. 39.
Popper, A. N., Hawkins, A. D., Fay, R. R., Mann, D. A., Bartol, S., Carlson, T. J., Coombs, S., Ellison, W. T., Gentry, R. L., Halvorsen, M. B., Løkkeborg, S., Rogers, P. H., Southall, B. L., Zeddies, D. G., and Tavolga, W. N. (**2014**). ASA S3/SC1. 4 TR-2014, "Sound exposure guidelines for fishes and sea turtles: A technical report prepared by ANSI-Accredited standards committee S3/SC1 and registered with ANSI" (Springer, New York).
Prior, M. K., Brown, D. J., and Haralabus, G. (**2011**). "Data features from long-term monitoring of ocean noise," in *4th International Conference and Exhibition on Underwater Acoustic Measurements: Technologies and Results*, Kos, Greece.
Prior, M. K., Brown, D. J., and Haralabus, G. (**2012**). "Data features from long-term monitoring of ocean noise," in *European Conference on Underwater Acoustics*, Edinburgh.
Richardson, W. J., Greene, C. R., Malme, C. I., and Thomson, D. H. (**1995**). *Marine Mammals and Noise* (Academic, San Diego), Chap. 1, 9–12.
Ross, D. (**2005**). "Ship sources of ambient noise," IEEE J. Ocean. Eng. **30**, 257–261.
Rouseff, D., and Tang, D. (**2010**). "Internal waves as a proposed mechanism for increasing ambient noise in an increasingly acidic ocean," JASA Express Lett. **127**, EL235–EL239.
Shipbuilders' Association of Japan (**2019**). "Shipbuilding_Statistics March 2019," from the Shipbuilders' Association of Japan, available at https://www.sajn.or.jp/files/view/articles_doc/src/addd344c6169359e87a5f39-d64e02173.pdf (last viewed 2019-08-30).
Sertlek, H. Ö., Slabbekoorn, H., ten Cate, C., and Ainslie, M. A. (**2019**). "Source specific sound mapping: Spatial, temporal and spectral distribution of sound in the Dutch North Sea," Environ. Pollut. **247**, 1143–1157.
Signorini, S. R., and McClain, C. R. (**2012**). "Subtropical gyre variability as seen from satellites," Remote Sens. Lett. **3**(6), 471–479.
Slabbekoorn, H., Bouton, N., van Opzeeland, I., Coers, A., ten Cate, C., and Popper, A. N. (**2010**). "A noisy spring: The impact of globally rising underwater sound levels on fish," Trends Ecol. Evol. **25**, 419–427.
Southall, B. L., Bowles, A. E., Ellison, W. T., Finneran, J. J., Gentry, R. L., Greene, C. R., Jr., Kastak, D., Ketten, D. R., Miller, J. H., Nachtigall, P. E., Richardson, W. J., Thomas, J. A., and Tyack, P. L. (**2007**). "Marine mammal noise exposure criteria: Initial scientific recommendations," Aquatic Mammals **33**(4), 411–521.
Southall, B. L., Finneran, J. J., Reichmuth, C., Nachtigall, P. E., Ketten, D. R., Bowles, A. E., Ellison, W. T., Nowacek, D. P., and Tyack, P. L. (**2019**). "Marine mammal noise exposure criteria: Updated scientific recommendations for residual hearing effects," Aquatic Mammals **45**(2), 125–232.
Udovydchenkov, I. A., Duda, T. F., Doney, S. C., and Lima, I. D. (**2010**). "Modeling deep ocean shipping noise in varying acidity conditions," J. Acoust. Soc. Am. **128**, EL130–EL136.
Van der Graaf, A. J., Ainslie, M. A., André, M., Brensing, K., Dalen, J., Dekeling, R. P. A., Robinson, S., Tasker, M. L., Thomsen, F., and Werner, S. (**2012**). "European Marine Strategy Framework Directive—Good Environmental Status (MSFD GES): Report of the Technical Subgroup on Underwater noise and other forms of energy."

https://doi.org/10.1121/10.0003960

van der Schaar, M., Ainslie, M. A., Robinson, S. P., Prior, M. K., and André, M. (**2014**). "Changes in 63 Hz third-octave band sound levels over 42 months recorded at four deep-ocean observatories," J. Mar. Syst. **130**, 4–11.
Wales, S. C., and Diachok, O. I. (**1981**). "Ambient noise vertical directionality in the northwest Atlantic," J. Acoust. Soc. Am. **70**, 577–582.
Wales, S. C., and Heitmeyer, R. M. (**2002**). "An ensemble source spectra model for merchant ship-radiated noise," J. Acoust. Soc. Am. **111**, 1211–1231.
Wang, H., Li, Y., Li, Q., and Yu, X. (**2019**). "Cluster analysis of deep water sound speed profiles in Indian Ocean," IOP Conf. Ser.: Earth Environ. Sci. **310**(5), p. 052048.
Wenz, G. (**1969**). "Low-frequency deep-water ambient noise along the Pacific Coast of the United States," U.S. Navy J. Underwater Acoust. **19**, 423–444.
Weston, D. E. (**1980**). "Ambient noise depth-dependence models and their relation to low-frequency attenuation," J. Acoust. Soc. Am. **67**, 530–537.
Wu, Z., Huang, N. E., Wallace, J. M., Smoliak, B. V., and Chen, X. (**2011**). "On the time-varying trend in global-mean surface temperature," Clim. Dyn. **37**(3–4), 759–773.
Yashayaev, I. M., and Zveryaev, I. I. (**2001**). "Climate of the seasonal cycle in the North Pacific and the North Atlantic oceans," Int. J. Climatol. **21**(4), 401–417.